

BOUSSINESQ MODELING OF WAVE TRANSFORMATION, BREAKING, AND RUNUP. I: 1D

By Andrew B. Kennedy,¹ Qin Chen,² James T. Kirby,³ and Robert A. Dalrymple⁴

ABSTRACT: Parts I and II of this paper describe the extension and testing of two sets of Boussinesq-type equations to include surf zone phenomena. Part I is restricted to 1D tests of shoaling, breaking, and runup, while Part II deals with two horizontal dimensions. The model uses two main extensions to the Boussinesq equations: a momentum-conserving eddy viscosity technique to model breaking, and a “slotted beach,” which simulates a shoreline while allowing computations over a regular domain. Bottom friction is included, using a quadratic representation, while the 2D implementation of the model also considers subgrid mixing. Comparisons with experimental results for regular and irregular wave shoaling, breaking and runup for both one and two horizontal dimensions show good agreement for a variety of wave conditions.

INTRODUCTION

It has long been a goal of coastal engineers to produce a computational wave model that is capable of accurately simulating wave motion from deep water through the surf zone. To do this, a model would have to include, among other things, nonlinear shoaling, refraction, diffraction, wave-wave interaction, breaking, and runup. As it is currently impractical to perform a full solution of the Navier-Stokes equations over any significant domain, approximate models must be used.

One set of candidate models is the various Boussinesq-type equations (Peregrine 1967; Madsen and Sørensen 1992; Nwogu 1993; Wei et al. 1995). These can describe, to varying degrees of accuracy in representing nonlinearity and dispersion, most phenomena exhibited by nonbreaking waves in finite depths. However, as derived, they do not include dissipation due to wave breaking and thus become invalid in the surf zone. Accordingly, there have been attempts to introduce wave breaking into Boussinesq models. Heitner and Housner (1970) introduced artificial viscosity terms into momentum conservation equations in order to capture the shock across a tsunami bore. These terms conserved overall momentum, which is very important for a breaking scheme. Tao (1983, 1984) used a crude nonconservative eddy viscosity term in order to model breaking. Zelt (1991) used an eddy viscosity formulation that was somewhat similar to that of Heitner and Housner together with a Lagrangian Boussinesq model to study the breaking and runup of solitary waves. However, in the conversion, the breaking term lost its momentum-conserving form. Using a roller-based approximation, Schäffer et al. (1993) and Madsen et al. (1997a) (referred to hereafter as DHI) have developed a comprehensive breaking and surf zone model based on a flux version of the Boussinesq equations which can model breaking phenomena such as wave height decay, wave-induced setup, and runup. Svendsen et al. (1996) developed a breaking wave model that consistently includes rotational effects caused by breaking in order to model dissipation. They also compared their model with the DHI roller

model and a precursor to the model described here (Wei and Kirby 1996) and found similarities in all three techniques.

This and Part II, a companion paper (Chen et al. 2000), document the extension of the fully nonlinear Boussinesq equations of Wei et al. (1995) and the extended Boussinesq equations of Nwogu (1993) to include surf zone phenomena related to wave breaking and runup. In this paper, the surf zone model is introduced and its performance for 1D breaking and runup is examined. Part II (Chen et al. 2000) considers surf zone modeling for two horizontal dimensions. An additional, related paper considers the Boussinesq modeling of a rip current system (Chen et al. 1999).

The basis of the breaking scheme used here is a simple eddy viscosity-type model, in contrast to some of the more complicated techniques available. This is somewhat like the eddy viscosity formulation of Heitner and Housner (1970) or Zelt (1991), but with extensions to provide a more realistic description of the initiation and cessation of wave breaking. Comparisons are made with laboratory results for 1D breaking and shoreline runup, with generally good results. The shoreline is treated using an improved version of the slot method described by Tao (1983, 1984).

SURF ZONE MODEL

Breaking Model

Both the extended Boussinesq equations of Nwogu (1993) and Wei et al. (1995), (referred to hereafter as WKGS) are written in terms of a reference velocity $\mathbf{u}_\alpha = (u_\alpha, v_\alpha)$ at some reference elevation z_α . The WKGS equation for conservation of mass may be written as

$$\eta_t + \nabla \cdot \mathbf{M} = 0 \quad (1)$$

where h is the still water depth, η is the free surface elevation, and

$$\mathbf{M} = (h + \eta) \left[\mathbf{u}_\alpha + \left(\frac{z_\alpha^2}{2} - \frac{1}{6} (h^2 - h\eta + \eta^2) \right) \nabla (\nabla \cdot \mathbf{u}_\alpha) + \left[z_\alpha + \frac{1}{h} (h - \eta) \right] \nabla (\nabla \cdot (h\mathbf{u}_\alpha)) \right] \quad (2)$$

The associated momentum conservation equation is

$$\mathbf{u}_{\alpha t} + (\mathbf{u}_\alpha \cdot \nabla) \mathbf{u}_\alpha + g \nabla \eta + \mathbf{V}_1 + \mathbf{V}_2 = 0 \quad (3)$$

where g is the downwards gravitational acceleration and \mathbf{V}_1 and \mathbf{V}_2 are the dispersive Boussinesq terms:

$$\mathbf{V}_1 = \frac{z_\alpha^2}{2} \nabla (\nabla \cdot \mathbf{u}_{\alpha t}) + z_\alpha \nabla (\nabla \cdot (h\mathbf{u}_{\alpha t})) - \nabla \left[\frac{\eta^2}{2} \nabla \cdot \mathbf{u}_{\alpha t} + \eta \nabla \cdot (h\mathbf{u}_{\alpha t}) \right] \quad (4)$$

¹Postdoctoral Fellow, Ctr. for Appl. Coast. Res., Univ. of Delaware, Newark, DE 19716.

²Postdoctoral Fellow, Ctr. for Appl. Coast. Res., Univ. of Delaware, Newark, DE.

³Prof., Ctr. for Appl. Coast. Res., Univ. of Delaware, Newark, DE.

⁴Prof. and Dir., Ctr. for Appl. Coast. Res., Univ. of Delaware, Newark, DE.

Note. Discussion open until July 1, 2000. Separate discussions should be submitted for the individual papers in this symposium. To extend the closing date one month, a written request must be filed with the ASCE Manager of Journals. The manuscript for this paper was submitted for review and possible publication on January 28, 1999. This paper is part of the *Journal of Waterway, Port, Coastal, and Ocean Engineering*, Vol. 126, No. 1, January/February, 2000. ©ASCE, ISSN 0733-950X/00/0001-0039-0047/\$8.00 + \$.50 per page. Paper No. 20144.

$$\mathbf{V}_2 = \nabla \left[(z_\alpha - \eta)(\mathbf{u}_\alpha \cdot \nabla)(\nabla \cdot (h\mathbf{u}_\alpha)) + \frac{1}{2}(z_\alpha^2 - \eta^2)(\mathbf{u}_\alpha \cdot \nabla)(\nabla \cdot \mathbf{u}_\alpha) \right] + \frac{1}{2} \nabla [(\nabla \cdot (h\mathbf{u}_\alpha)) + \eta \nabla \cdot \mathbf{u}_\alpha]^2 \quad (5)$$

Nwogu's equations are recovered by neglecting nonlinear dispersive terms. The mass conservation equation remains in the form of (1), but with

$$\mathbf{M} = (h + \eta)\mathbf{u}_\alpha + \left(\frac{hz_\alpha^2}{2} - \frac{h^3}{6} \right) \nabla(\nabla \cdot \mathbf{u}_\alpha) + \left(hz_\alpha + \frac{h^2}{2} \right) \nabla(\nabla \cdot (h\mathbf{u}_\alpha)) \quad (6)$$

while the equation for momentum conservation becomes

$$\mathbf{u}_{\alpha t} + (\mathbf{u}_\alpha \cdot \nabla)\mathbf{u}_\alpha + g\nabla\eta + \frac{z_\alpha^2}{2} \nabla(\nabla \cdot \mathbf{u}_{\alpha t}) + z_\alpha \nabla(\nabla \cdot (h\mathbf{u}_{\alpha t})) = 0 \quad (7)$$

Linear dispersion properties vary with the choice of z_α . Nwogu (1993) describes an error-minimizing condition that, when applied to the range $0 < kh < \pi$, yields the result $z_\alpha = -0.531h$, which will be used in all calculations.

The above equations are only valid for nonbreaking waves, so some additional approximation must be made to model wave breaking. In contrast to some of the more complicated methods mentioned earlier, a simple eddy viscosity-type formulation is used to model the turbulent mixing and dissipation caused by breaking. The mass conservation equation (1) remains unchanged, while, with the additional eddy viscosity terms, the equation for momentum conservation becomes

$$\mathbf{u}_{\alpha t} + \dots - \mathbf{R}_b = 0 \quad (8)$$

where

$$\mathbf{R}_{bx} = \frac{1}{h + \eta} \left([v(h + \eta)u_{\alpha x}]_x + \frac{1}{2} [v(h + \eta)u_{\alpha y}]_y + v((h + \eta)v_{\alpha x})_y \right) \quad (9)$$

$$\mathbf{R}_{by} = \frac{1}{h + \eta} \left([v(h + \eta)v_{\alpha y}]_y + \frac{1}{2} [v(h + \eta)u_{\alpha x}]_x + v((h + \eta)v_{\alpha x})_x \right) \quad (10)$$

By multiplying the momentum equations by $h + \eta$ and integrating over a breaking event, these additional terms may be shown to conserve overall momentum. The model behavior is thus consistent (in the region of a breaking wave crest) with the momentum-conserving bore process in open-channel flow.

The eddy viscosity v , which is a function of both space and time, is determined in a similar manner to Zelt (1991), but with several differences. The eddy viscosity is given here by

$$v = B\delta_b^2(h + \eta)\eta_t \quad (11)$$

where δ_b is a mixing length coefficient. From the results of many tests, it is set here to a dimensionless value of $\delta_b = 1.2$. Surprisingly, computations are relatively insensitive to changes in this parameter, and values between 0.9 and 1.5 were found to give very similar results. The quantity B varies smoothly from 0 to 1 so as to avoid an impulsive start of breaking and the resulting instability. It is given by

$$B = \begin{cases} 1, & \eta_t \geq 2\eta_t^* \\ \frac{\eta_t}{\eta_t^*} - 1, & \eta_t^* < \eta_t \leq 2\eta_t^* \\ 0, & \eta_t \leq \eta_t^* \end{cases} \quad (12)$$

The parameter η_t^* determines the onset and cessation of breaking. Use of η_t as an initiation parameter ensures in a simple manner that the dissipation is concentrated on the front face of the wave, as in nature. Zelt (1991) assumed that parameters of this sort would have a constant value, but this is not in accordance with reality. For example, in nature, spilling and plunging ocean waves do not begin to break until the wave overturns, but once the wave has broken, it will continue to break until it either reaches the beach or arrives at some smaller stable level at which it will reform (Horikawa and Kuo 1966). A similar assumption was used in the breaking model of Schäffer et al. (1993). In the present model, a breaking event begins when η_t exceeds some initial threshold value, but, as breaking develops, the wave will continue to break even if η_t drops below this value. The magnitude of η_t^* therefore, decreases in time from some initial value $\eta_t^{(i)}$ to a terminal quantity $\eta_t^{(f)}$. No strong evidence exists for what form this decrease would take, so a simple linear relation is used here to model the evolution of η_t^* . This becomes

$$\eta_t^* = \begin{cases} \eta_t^{(f)}, & t \geq T^* \\ \eta_t^{(i)} + \frac{t - t_0}{T^*}(\eta_t^{(f)} - \eta_t^{(i)}), & 0 \leq t - t_0 < T^* \end{cases} \quad (13)$$

where T^* is the transition time, t_0 is the time that breaking was initiated, and thus $t - t_0$ is the age of the breaking event, which is nonnegative. The default values of $\eta_t^{(i)}$ and $\eta_t^{(f)}$ used here are $0.65\sqrt{gh}$ and $0.15\sqrt{gh}$, respectively. The default transition time used here is $T^* = 5\sqrt{h/g}$. None of these quantities may be regarded as universal values; they were chosen on the basis of multiple tests with different parameter values to give good agreement with experimental measurements for the WKGS and Nwogu equations. For use in other Boussinesq models with different linear and nonlinear performance, care must be taken to ensure that these parameters are appropriate.

In fact, even the form of the breaking initiation criterion is somewhat arbitrary. For spilling and plunging ocean waves, breaking initiates when crests overturn, a condition that can never occur in a Boussinesq model. Therefore, the approximate criterion η_t^* was chosen here, but other possible criteria include the slope of the water surface used by Schäffer et al. (1993) or the gradient or curvature of the reference velocity \mathbf{u}_α . Each has advantages and disadvantages when compared to the others. Two advantages of using η_t^* are that the quantity η_t is already known from normal Boussinesq computations, and stability is good when compared to other schemes tested. The largest disadvantage is that, in some special cases, such as stationary hydraulic jumps, the criterion may be Doppler-shifted to the point where breaking initiation is not recognized.

For wave motion in one horizontal dimension, breaking events are well defined. The quantity t_0 , the time when breaking was initiated, will in general vary for different breaking events within a system, but it is a simple matter to track any particular event as it progresses toward the shore, and thus to know the age of each event. For example, in the outer surf zone, a wave may have begun breaking a short time before the present. The age of breaking $t - t_0$ will thus be small, and η_t^* will be slightly less than $\eta_t^{(i)}$. However, at the same time, there may be another breaking event in the inner surf zone, where $t - t_0 > T^*$ and thus $\eta_t^* = \eta_t^{(f)}$.

For all breaking events, the eddy viscosity, v , is filtered for stability using a three-point filter before it is inserted into (9)–(10).

For two horizontal dimensions, the problem becomes slightly more difficult and is detailed in Part II (Chen et al. 2000).

Moving Shoreline

For computations of wave runup, and for computing wave motion over natural coasts, it is necessary for a wave model

to be able to simulate the land-sea interface realistically. To do this, a modification of the slot method of Tao (1983, 1984) is used. In this, the entire computational domain is considered active, but where there is very little or no water covering the land, modified equations are solved. These equations assume that, instead of being solid, the beach is porous, or contains narrow "slots," so it is possible for the water level to be below the beach elevation. Alternatively, this method may be thought of as a "thin film" technique with a modified gravitational term, in which a very thin layer of water covers "dry" areas.

Madsen et al. (1997a,b) utilized a variant of the slot technique in an extended Boussinesq model formulated in terms of volume flux and free surface elevation and demonstrated the effectiveness of the slot method for simulation of wave runup on beaches. Although the agreement between the modeled and measured swash motions on sloping fixed beds at laboratory scales was shown to be reasonably good by Madsen et al. (1997a), a comparison with the analytical solution of wave runup on a solid slope (Carrier and Greenspan 1958) indicated that the slot method tended to underpredict the maximum runup height with about a 10% error, even when a very narrow slot width was used. This was because, before water could cover a previously dry area, the slot first needed to be filled, decreasing slightly the overall volume available for runup. Because the maximum runup height is very sensitive to the total volume at the runup tip, runup is underpredicted. Thus, a slightly different formulation is proposed that ensures that, when the water level is above the top of the slot, there will be no net fluid loss at that location. Some small mass loss still exists from water flowing into the slots where the water level is below the top of the slot, but it is much reduced.

Fig. 1 shows a schematic of a wave flume with a sloping bottom in the presence of a narrow slot. The width of the wave flume is defined as

$$b(\eta) = \begin{cases} 1, & \eta \geq z^* \\ \delta + (1 - \delta)e^{\lambda(\eta - z^*)/h_0}, & \eta \leq z^* \end{cases} \quad (14)$$

in which δ is the slot width relative to a unit width of beach; λ is the shape parameter that controls the smooth transition of the cross-sectional area from a unit width to a narrow slot; z^* denotes the elevation of the seabed where $b = 1$; h_0 is a reference water depth that must be deeper than the water depth at the lower limit of the swash zone; and η is the free surface elevation relative to the still water level. Thus the cross-sectional area of the channel can be expressed by

$$A(\eta) = \begin{cases} (\eta - z^*) + \delta(z^* + h_0) + \frac{(1 - \delta)h_0}{\lambda} (1 - e^{-\lambda(1+z^*/h_0)}), & \eta \geq z^* \\ \delta(\eta + h_0) + \frac{(1 - \delta)h_0}{\lambda} e^{\lambda(\eta - z^*)/h_0} (1 - e^{-\lambda(1+\eta/h_0)}), & \eta \leq z^* \end{cases} \quad (15)$$

The equation for conservation of mass in the wave channel is

$$A_t + (AU)_x = 0 \quad (16)$$

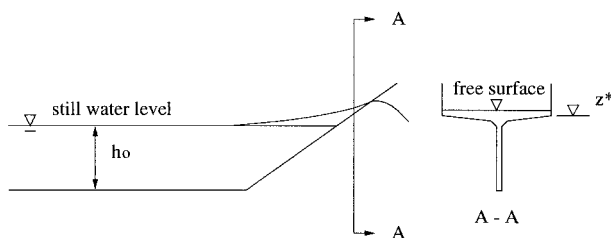


FIG. 1. Schematic of Channel with Presence of Narrow Slot

where U is the depth-averaged velocity. Omitting the effect of a narrow slot on the vertical distribution of the fluid particle velocity in the wave flume leads to the mass equation formulated in terms of the velocity at the reference level z_α as follows

$$\beta \eta_t + M_x = 0 \quad (17)$$

in which

$$M = \Lambda \left[u_\alpha + \left(\frac{z_\alpha^2}{2} - \frac{1}{6} (h^2 - h\eta + \eta^2) \right) u_{\alpha,xx} + \left(z_\alpha + \frac{1}{2} (h - \eta) \right) (hu_{\alpha,xx}) \right] \quad (18)$$

Here $\beta = b(\eta)$ and $\Lambda = A(\eta)$. Eqs. (17)–(18) will replace the 1D version of (1) and (2) for the simulation of wave runup using the slot technique. Since the presence of a narrow slot does not alter the momentum equations formulated in terms of velocity and surface elevation, the extension of this treatment of a moving shoreline to the case of two horizontal dimensions is straightforward. For detailed 2D applications, the reader is referred to Part II (Chen et al. 2000).

The fulfillment of mass conservation in the presence of an artificial slot depends on the choice of z^* in the functions β and Λ . In Tao's (1984) and Madsen et al.'s (1997a) formulation, z^* is chosen to be $z = -h$, the elevation of the physical solid seabed. This leads to an effective loss of mass during runup, as water must first fill the slots before it can wet the dry beach face. The opposite phenomenon occurs during run-down. Here, we choose z^* by specifying that, once the water level is above the top of the slot, the overall volume will be identical to that if it would have if no slot existed. For $\eta \geq z^*$, equating the cross-sectional area with and without a slot leads to

$$\eta - z^* + \delta(z^* + h_0) + \frac{(1 - \delta)h_0}{\lambda} (1 - e^{-\lambda(1+z^*/h_0)}) = \eta + h \quad (19)$$

For $\delta \ll 1$ and $\lambda \gg 1$, the elevation at the top of the slot, z^* , will be near $z = -h$. Thus, using a Taylor series expansion of $\exp(-\lambda(1 + z^*/h_0))$ about $z = -h$, and neglecting second-order and higher terms, we get

$$z^* = \frac{\delta h_0 - h}{(1 - \delta)(1 - e^{-\lambda(1-h/h_0)})} + \frac{h_0}{\lambda} - \frac{h}{1 - e^{\lambda(1-h/h_0)}} \quad (20)$$

Since $\lambda \gg 1$ as used in practice, (20) can be simplified as

$$z^* = \frac{-h}{1 - \delta} + h_0 \left(\frac{\delta}{1 - \delta} + \frac{1}{\lambda} \right) \quad (21)$$

The choice of z^* as defined in (20) or (21) will lead to improvement in the prediction of maximum runup height, as shown in the following section, where we shall discuss the optimal values of δ and λ .

MODEL VERIFICATION

Wave Breaking

To test performance of the breaking model, results were compared to regular and irregular wave breaking experiments. Comparisons began with a series of 1D regular wave tests on plane slopes. Five tests were chosen out of a large series performed by Hansen and Svendsen (1979), for conditions ranging from spilling to plunging breakers. Here, both experimental and computational wave generators added a second harmonic to the input signals, with amplitude and phase empirically chosen to minimize free second harmonics. Next, Run

2 of the irregular wave tests of Mase and Kirby (1992) was simulated. In addition to wave heights, time series of surface elevation and a wide range of statistical parameters were compared for these tests. For both sets of tests, the breaking parameters were set to the values given in the section on the breaking model, and slot values were set to $\lambda = 80$ and $\delta = 0.005$.

Regular Waves

Hansen and Svendsen (1979) reported on a large series of shoaling and breaking tests involving regular waves. Waves were generated on a horizontal bottom at a depth of 0.36 m, shoaled, and broke on a 1:34.26 planar slope. Measurements of surface elevation were taken at a very large number of locations using an automated, continuously moving trolley. For the purposes of the present study, computed wave heights and setups were compared with the measured values, both seaward of and inside the surf zone.

Because of the moving trolley used in the experiment and the correspondingly small sample size at any particular location, measurements showed considerable scatter, especially in the surf zone. For this study, they were therefore smoothed somewhat by averaging the results at any three adjacent measurement locations, and rounding to the nearest millimeter for wave heights and 0.1 mm for setup. Since the measurement locations were typically separated by only a few centimeters, the evolution of a wave between adjacent locations was usually insignificant, while the averaging process reduced scatter considerably. Even with this reduction of data, there were still hundreds of measurements for each wave condition, so the data set was further reduced to approximately 40–45 per wave, which gave a good description of the wave shoaling and breaking. Further, Hansen and Svendsen's estimates of overall water volume showed that "a certain amount of water seems to be pumped to the inactive part of the flume behind the sloping bottom during the test." This resulted in a decrease in mean water level over the active part of the flume. To compensate for this loss of water, and because the experimental and computational wave tanks had different total volumes, small offsets were applied here to some of the experimental runs to match computed values of setdown in the deeper part of the tank.

Five cases were simulated here, covering a wide range of breaker types, and serving as a necessary initial test for the surf zone model. Table 1 lists characteristics for all waves tested. Breaker types are based on a surf similarity analysis, initial wave numbers are computed from linear theory, and wave numbers at breaking are taken from Hansen and Svendsen (1979).

The first test, case 031041 as defined in Table 1, was well into the plunging regime. Fig. 2 shows computed and measured wave heights as the wave propagates up the slope. Heights using the WKGS and Nwogu equations are reasonable as the wave shoals and breaks. However, both sets of equations appear to slightly underpredict the peak wave height at breaking. The setup trend is predicted well. For this and many of the other waves tested, some backward-propagating short wave noise was generated during breaking. This had the effect of increasing the measured crest-to-trough height, both in the surf zone and offshore. For this particular test, this meant that matching wave heights offshore may have led to an underestimate of the primary wave height and the consequent under-shoaling. This test also shows clearly one of the two most significant sources of error: wave heights in the inner surf zone tend to be overpredicted.

The next breaker, case 041041, was somewhat shorter and was near the plunging-spilling transition. Fig. 3 shows computed and measured wave evolution and setup. Once again,

TABLE 1. Experimental Wave Parameters for Hansen and Svendsen Tests

Case (1)	T (s) (2)	H_0 (cm) (3)	Breaker type (4)	$kh_{(I)}$ (5)	$kh_{(B)}$ (6)
031041	3.33	4.3	Plunging	0.369	0.18
041041	2.5	3.9	Spilling-plunging	0.501	0.24
051041	2.0	3.6	Spilling	0.641	0.27
061071	1.67	6.7	Spilling	0.791	0.41
A10112	1.0	6.7	Spilling	1.58	0.76

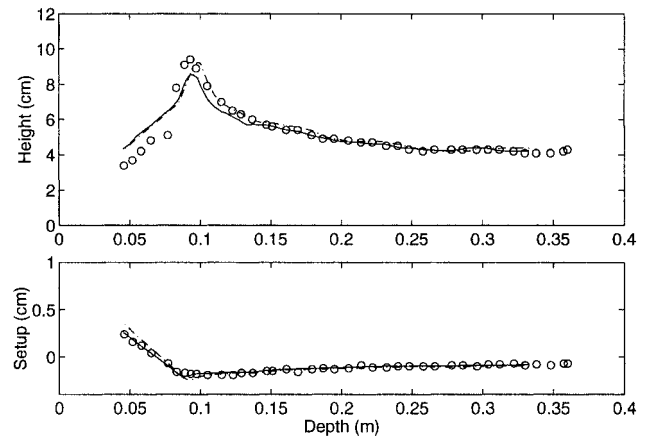


FIG. 2. Computed and Measured Wave Heights and Setup for Hansen and Svendsen Plunging Breaker 031041: Data (○); WKGS (—); Nwogu (---)

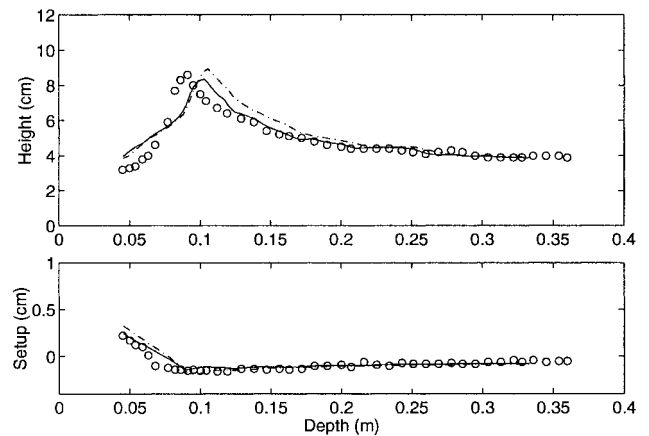


FIG. 3. Computed and Measured Wave Heights and Setup for Hansen and Svendsen Spilling-Plunging Breaker 041041: Data (○); WKGS (—); Nwogu (---)

the WKGS equations give a good description of wave shoaling and breaking, although wave heights are slightly overpredicted as the wave shoals, and thus the computational wave breaks slightly early. Computations using Nwogu's equations show a similar trend, although the overshooting is further exaggerated. Comparing setup, both sets of Boussinesq equations give good results, although setup begins slightly early, which follows directly from the error in the breakpoint location.

Fig. 4 shows computed and measured wave heights for case 051041. This shows a trend similar to the previous case. Wave shoaling is again predicted moderately well, but with overshooting. Wave induced setup for this case also appears reasonable, but a small difference in setdown slope may be discerned.

The observed overshooting was seen to some degree in most tests and is believed to be a result of the tendency of the WKGS and Nwogu equations to overpredict the magnitude of nonlinear superharmonics somewhat in intermediate depths.

For long waves, the WKGS equations provide very good predictions of solitary wave shoaling to near the breaking limit, while Nwogu's equations predict reasonable, though somewhat large, wave heights (Wei et al. 1995, Figs. 4–5). However, for waves in intermediate depth, nonlinear errors increase for both sets of equations. Fig. 5.3 in Madsen and Schäffer (1998) shows that for dimensionless wave numbers of $kh < 1.5$, which is approximately the range considered in these tests, Nwogu's equations show a maximum of about 20% overprediction in the bound second harmonic of a second-order steady wave. In

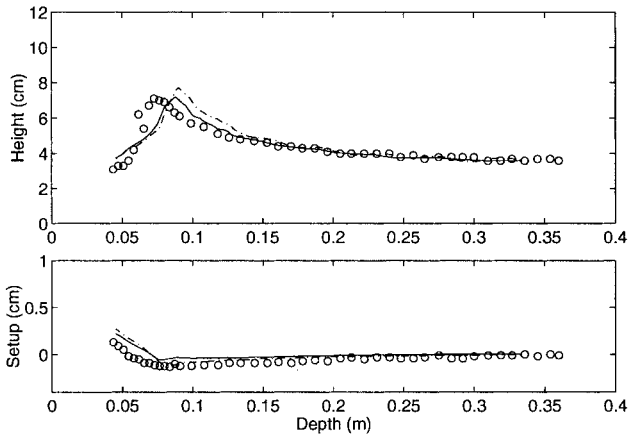


FIG. 4. Computed and Measured Wave Heights and Setup for Hansen and Svendsen Spilling Breaker 051041: Data (○); WKGS (—); Nwogu (---)

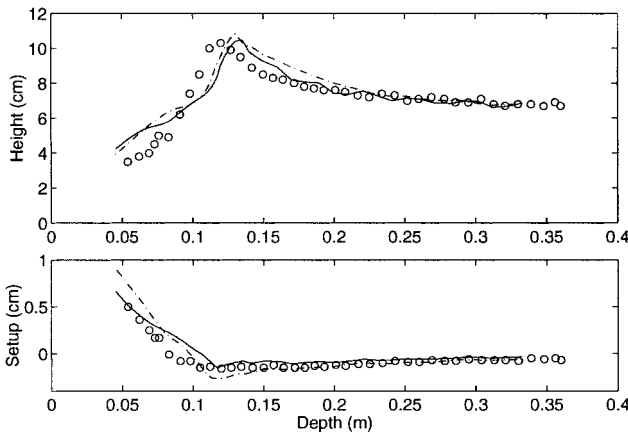


FIG. 5. Computed and Measured Wave Heights and Setup for Hansen and Svendsen Spilling Breaker 061071: Data (○); WKGS (—); Nwogu (---)

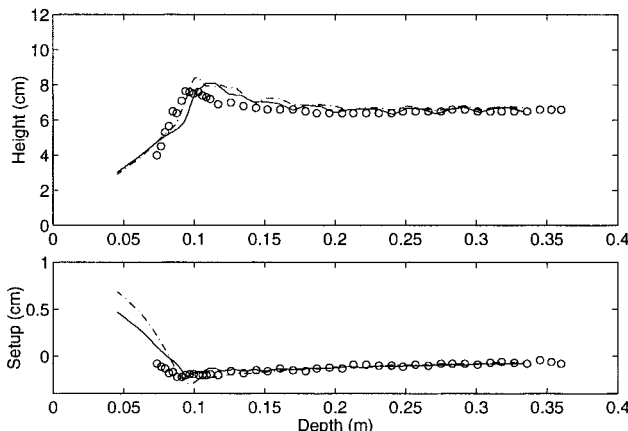


FIG. 6. Computed and Measured Wave Heights and Setup for Hansen and Svendsen Spilling Breaker A10112: Data (○); WKGS (—); Nwogu (---)

contrast, the WKGS equations have maximum errors of around 10% over this range. These bound second-order harmonics cannot cause overshooting; however, errors in third harmonics, which generally follow the trend of second-order solutions, will be noticed as over- or underpredictions of computed wave heights. This is believed to be the cause of the observed overshooting in some tests.

Fig. 5 shows computed wave heights for case 061071, which was another spilling breaker, with period 1.67 s and height 6.7 cm. Again, the trends are all very similar to the previous cases, with overshooting and somewhat premature breaking. Overall agreement for wave heights and setup appears to be comparable to the previous case. Once again, Nwogu's equations have a slightly worse prediction of setup than the WKGS equations shoreward of the break point.

The final wave tested from Hansen and Svendsen's tests was a spilling breaker with period 1.0 s and height 6.7 cm. This was designated case A10112. Fig. 6 shows wave heights. Once again, overshooting occurs, but agreement is better than the previous wave. No strong comparison may be made for setup in this case, as there are few data shoreward of the breakpoint. From the little available, computed setup using Nwogu's equations appears to increase somewhat more quickly after breaking than measured values.

Overall, although agreement is, on the whole, reasonable, some general error trends become clear. Wave heights in the inner surf zone are overpredicted, a trend that proved very robust to changes in the breaking parameters. It is unclear whether this result derives from the breaking model, the Boussinesq equations used, or some combination of the two.

Irregular Waves

For a test of model performance using irregular waves, the experiments of Mase and Kirby (1992) were simulated. Experiments were performed on a 1:20 planar slope using an incident Pierson-Moskowitz spectrum. Computational results were compared with data from Run 2, which had a peak frequency of 1.0 Hz and predominantly spilling breakers. Computations were initialized using a time series of data at the deepest measurement location, denoted wave gauge 1 in Fig. 7, which was assumed to represent linear, unidirectional waves. A small offset was added to the experimental data to match computed values of setdown at the deepest measurement location.

Fig. 8 shows a typical time series of computed and measured surface elevations at the other 11 wave gauges using the WKGS equations. Agreement is in general quite good, but deteriorates as the waves progress toward shore. This was to be expected, as the assumption of linear, unreflected incident waves used to generate the wave forms could only be an approximation to reality.

Overall statistical parameters can provide a more detailed picture of the breaking model performance. Fig. 9 shows standard deviations of measured and computed surface elevation and wave setup. Agreement is reasonable, although, once

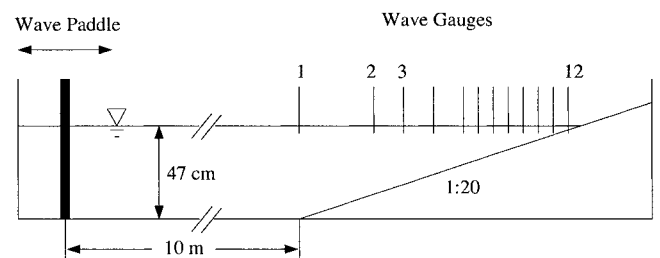


FIG. 7. Schematic View of Experimental Setup in Mase and Kirby (1992)

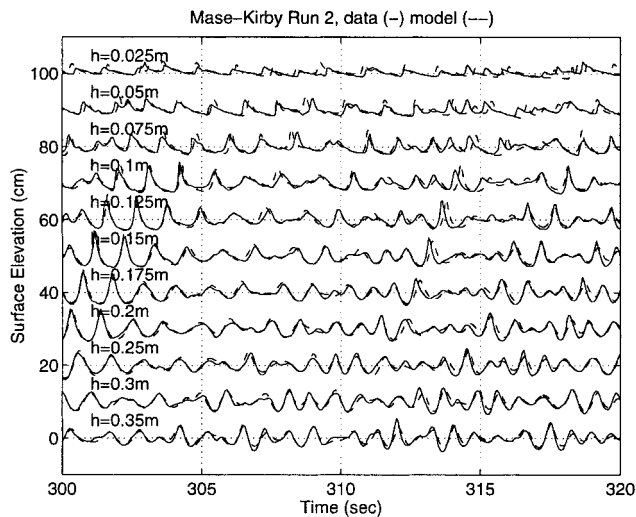


FIG. 8. Time Series of Surface Elevations for Mase and Kirby (1992) Run 2, Data (—), Computations (---)

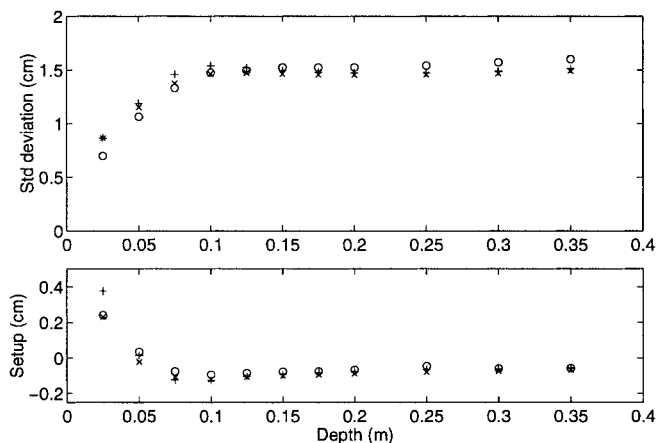


FIG. 9. Computed and Measured Standard Deviations of Surface Elevation and Setup for Mase and Kirby (1992) Run 2; Data (○), WKGS (×); Nwogu (+)

again, wave heights near the shoreline become too large. Computed setup appears quite good, especially using the WKGS equations.

Wave asymmetry, a measure of left–right differences in a wave, and skewness, a measure of crest–trough shape, are computed from time series of surface elevation at chosen locations, and are shown in Fig. 10. Asymmetry is defined as

$$As = \frac{\langle H(\eta)^3 \rangle}{\langle \eta^2 \rangle^{3/2}} \quad (22)$$

where H denotes the Hilbert transform, $\langle \rangle$ is the mean operator, and the mean has been removed from the time series of surface elevation. Skewness is defined as

$$Sk = \frac{\langle \eta^3 \rangle}{\langle \eta^2 \rangle^{3/2}} \quad (23)$$

using the zero mean surface elevation. Asymmetry is seen to increase steadily as the wave approaches the shoreline, corresponding to the well-known steep front and gentle back slopes of highly nonlinear shoaling and breaking waves. Both sets of Boussinesq equations predict this parameter very well. The trend of wave skewness is also predicted well, increasing as the wave shoals and breaks, and then decreasing near the shoreline. Positive skewness here corresponds to narrow crests and flat troughs. Both sets of equations tend to slightly overpredict maximum skewness, likely because of the tendency toward overshooting noted earlier.

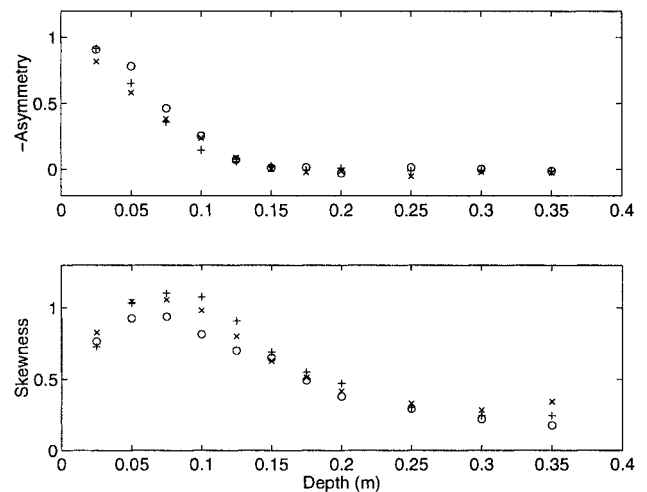


FIG. 10. Computed and Measured Wave Asymmetry and Skewness for Mase and Kirby (1992) Run 2; Data (○), WKGS (×); Nwogu (+)

Wave Runup

Nonbreaking Long Waves

A standard test of a numerical scheme for shoreline runup is the solution of a nonlinear long wave on a sloping bottom. Carrier and Greenspan (1958) provided an analytical solution that was reproduced closely by Özkan-Haller and Kirby (1997) using a numerical model based on a Fourier-Chebyshev collocation method. We shall verify our numerical results against those computed by Özkan-Haller and Kirby's model.

For convenience of comparison, the test case of a nonbreaking long wave on an impermeable slope as used by Madsen et al. (1997a) is repeated here. We consider a 10 s wave train with an initial wave height of 0.006 m in a wave channel containing a 1:25 slope. In the flat portion of the channel, the still-water depth is 0.5 m. Wave runup and rundown on the slope result in a standing wave form in the channel. Figs. 11(a and b) show the comparison of the spatial and temporal variations of the free surface and the horizontal shoreline motion computed by the present model with the slot technique and by Özkan-Haller and Kirby's (1997) model. The full lines represent the present results. We notice that the improved slot scheme as described in the preceding section predicts well the maximum runup height and surface depression, as well as the standing wave form in comparison with the exact solution denoted by the dashed lines. A slight deviation is observed, however, in the antinodal free surface displacement between the first two nodes and the peak of the horizontal shoreline motion because of the approximate nature of the slot scheme. In this simulation, δ and λ are chosen to be 0.002 and 80, respectively. As suggested by Madsen et al. (1997a), a filter localized in the swash zone on the basis of a five-point weighted average is also used in order to suppress noise near the shoreline due to the use of the slot. We chose the grid size and time step to be 0.1 m and 0.04 s, respectively. The Boussinesq terms are also switched off for consistency with the nonlinear shallow-water equations.

The improvement in the prediction of maximum shoreline excursion by the corrected slot scheme retaining mass conservation is illustrated by Fig. 11(c). In the figure, two curves respectively represent the computed maximum shoreline excursion as a function of the slot width taken relative to a unit width of beach by the use of the new and original definitions of z^* . We normalized the computed maximum shoreline excursion by the exact solution. The circles denote the numerical results of the present runup scheme with equivalent cross-sec-

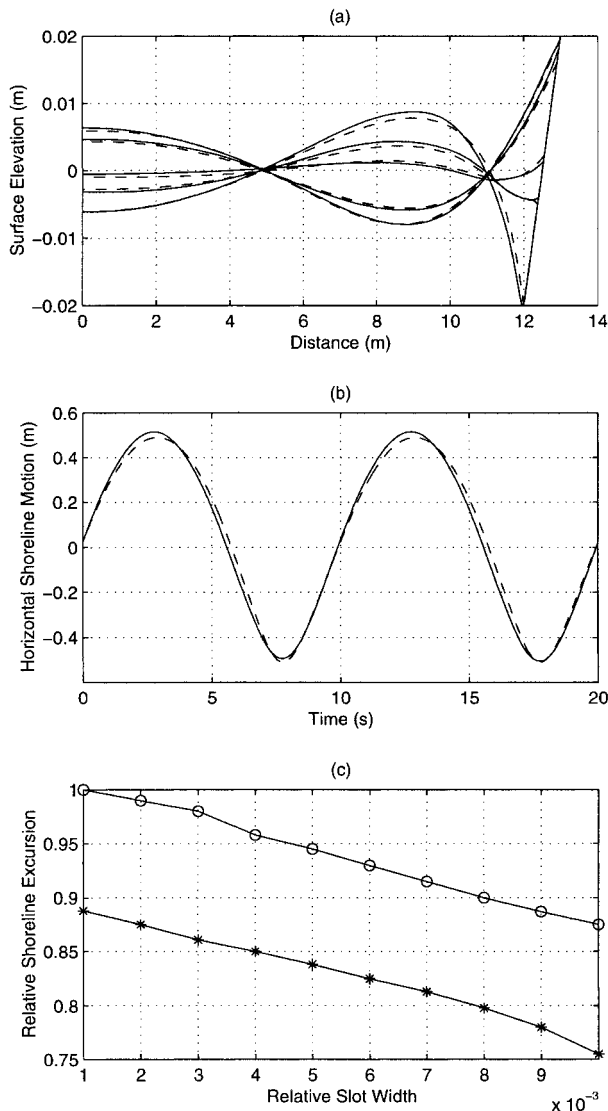


FIG. 11. (a) Free Surface Computed by Present Model (—) and by Özkan-Haller and Kirby's (1997) Model (---). (b) Computed Horizontal Shoreline Runup (—) and Özkan-Haller and Kirby's Model Result (---). (c) Convergence Rate of Maximum Shoreline Excursion Predicted by Improved and Original Slot Schemes. (O): Improved; (*): Original

tional area, while the stars are those using Tao's (1983) or Madsen et al.'s (1997a) scheme. Apparently, the proposed correction leads to much faster convergence in comparison with the results based on the original version of the slot technique. For example, with $\delta = 0.005$ and $\lambda = 80$, the improved slot scheme predicts the maximum runup height with less than 5% error, while the original one gives about 15% error in this test case.

Bichromatic Waves

In a study of frequency downshift in the swash motion, Mase (1995) presented experimental results of bichromatic wave train runup on a slope. The experiments were conducted using the same wave flume and experimental setup as those in Mase and Kirby (1992), described in the preceding section. Mase's laboratory measurements, including shoaling, breaking and swash motion, provide good test cases for the verification of the runup scheme in combination with the wave-breaking model.

We chose two typical test cases from Mase's (1995) series of experiments. Each of them represents a different kind of

wave group pattern. The first one, named WP1, contains 5 waves in each wave group with a mean frequency $f = 0.6$ Hz, while in the second case, WP2, each wave group consists of 10 waves with $f = 1.2$ Hz. In both cases, the nonlinear interactions of wave components and the variation of breaking point in the wave train, among others, cause considerable low-frequency swash oscillations. Unlike the simulation of Mase and Kirby's (1992) experiment, we use the Boussinesq model incorporating the improved slot scheme and the breaking model to simulate these two test cases.

Incident waves are generated using the source function technique developed by Wei et al. (1999). The measured time series of the free surface at Gauge 1 near the toe of the slope is used as an input to the model. As in the physical experiment, no effort is made to include bound second harmonics in the incident waves. Due to the presence of the slot inside the dry beach, the whole channel is an active computational domain with closed boundaries at each end of the wave flume. To be able to resolve superharmonics in the wave train, the grid size and the time step are chosen to be 0.02 m and 0.01 s, respectively. With respect to the wave-breaking model, the parameters are kept the same as those in the preceding simulations. For the slot scheme, we use $\delta = 0.005$, and $\lambda = 80$.

Comparisons of computed and measured surface elevation for the two test cases are presented in Figs. 12 and 13, including 11 wave gauges along the slope and a runup gauge. The dashed lines represent the computed results, while the full lines are the measurements. Generally good agreement is found in both test cases.

First, we notice that the nonlinear shoaling of the bichro-

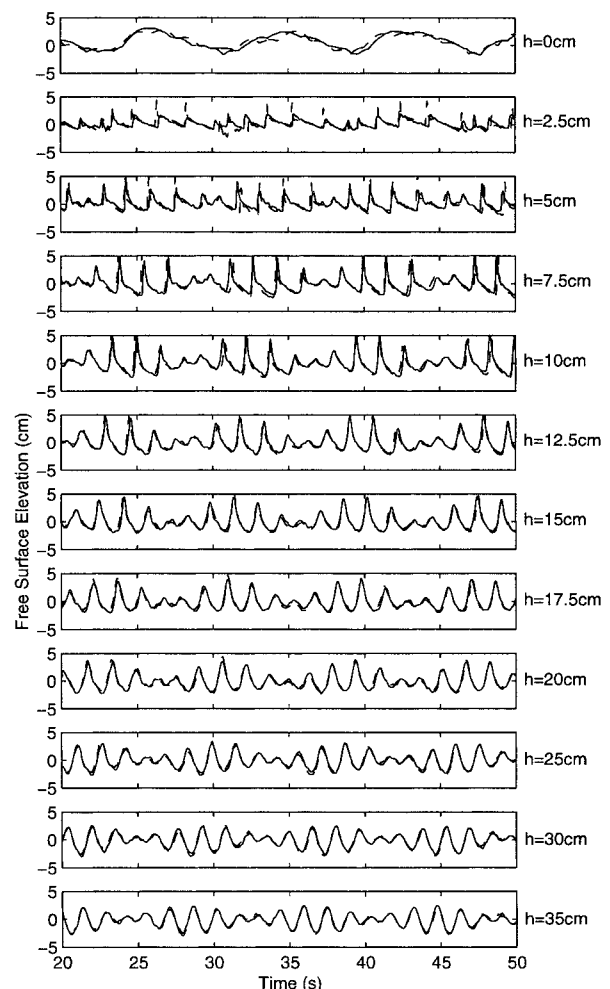


FIG. 12. Computed (---) and Measured (—) Free Surface Elevation Including Runup in Case WP1

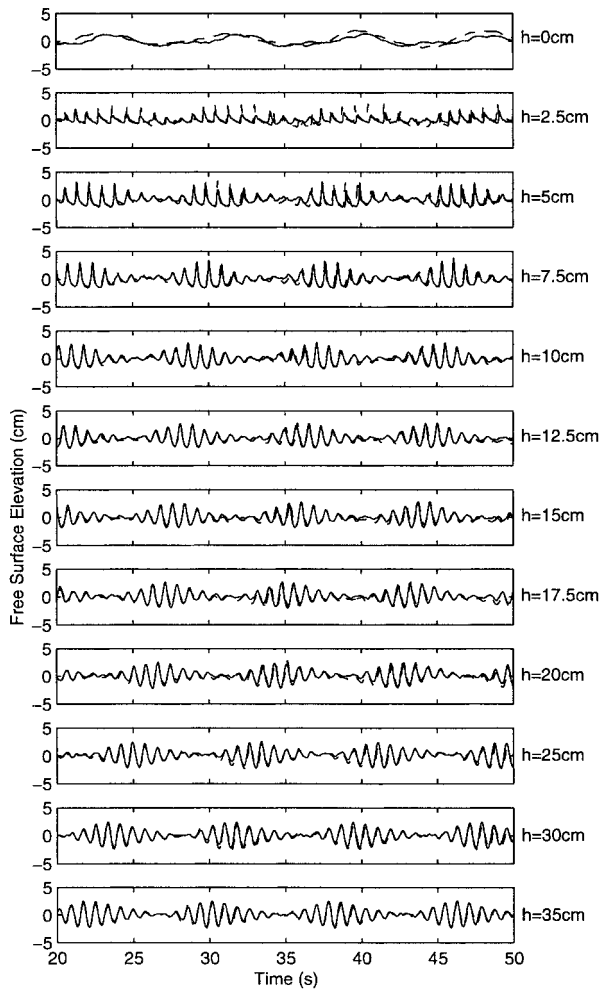


FIG. 13. Computed (---) and Measured (—) Free Surface Elevation Including Runup in Case WP2

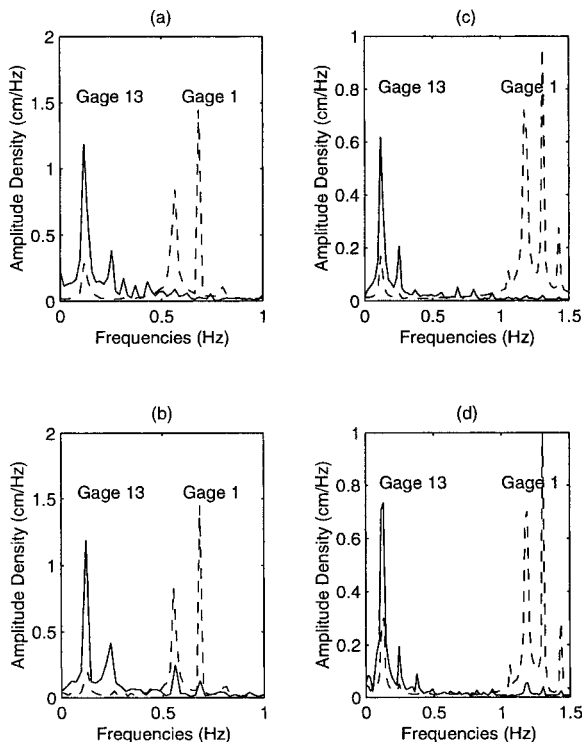


FIG. 14. Measured [(a) and (c)] and Computed [(b) and (d)] Frequency Downshift of Swash Motion. (a) and (b): Case WP1; (c) and (d): Case WP2

matic wave trains is well predicted by the Boussinesq model. Near the shoreline where wave breaking occurs, although a slight discrepancy is observed, the overall agreement is satisfactory between the computed surface elevation and Mase's (1995) data. Moreover, the modeled swash motions are in good agreement with the measurements. The frequency downshift of the swash motion in comparison with the frequency of the incoming waves is well reproduced by the present model, as illustrated in Fig. 14, where dashed lines denote the amplitude spectra offshore (Gauge 1), while solid lines are those in the swash zone (Gauge 13). The good agreement demonstrates that the present Boussinesq model with the incorporation of the wave-breaking model and the improved slot techniques works reasonably well for the simulation of wave shoaling, breaking, and swash oscillation. Similar successful simulations of wave breaking and runup were reported by Madsen et al. (1998b), who utilized a Boussinesq model based on the weakly nonlinear equations, a "roller"-type breaking scheme, and a similar treatment of the shoreline runup.

DISCUSSION AND CONCLUSIONS

A surf zone model has been developed for the fully nonlinear Boussinesq equations of Wei et al. (1995) and extended Boussinesq equations of Nwogu (1993), using a modified eddy viscosity model and a slot technique to represent the moving shoreline and dry land. Comparisons with experimental data show generally good agreement, although systematic differences do exist.

The model has shown itself to accurately predict wave transformation in the surf and swash zone. Breaking phenomena are predicted both qualitatively and quantitatively for a variety of 1D tests. Of all tests, the greatest errors are seen for monochromatic wave shoaling and breaking on a planar beach. Here, waves heights are somewhat overpredicted before breaking. This overprediction of shoaling waves appears to be due to the intrinsic nature of the Boussinesq equations used, which show nonlinear error in intermediate depths. Further work with higher-order equations may be needed to resolve this drawback. Runup tests, on the other hand, show good agreement with experimental results for all cases considered, although again some error is visible.

ACKNOWLEDGMENTS

This study has been supported by the Office of the Naval Research, Base Enhancement, through research grant N00014-97-1-0283. Many thanks are due to I. A. Svendsen and H. Mase, who provided the experimental data, and H. T. Özkan-Haller, who provided the runup solution, for comparisons.

APPENDIX. REFERENCES

- Carrier, G. F., and Greenspan, H. P. (1958). "Water waves of finite amplitude on a sloping beach." *J. Fluid Mech.*, Cambridge, England, 4, 97–109.
- Chen, Q., Kirby, J. T., Dalrymple, R. A., Kennedy, B. A., and Chawla, A. (2000). "Boussinesq modelling of wave transformation, breaking, and runup. II: 2D." *J. Wtrwy., Port, Coast., and Oc. Engrg.*, ASCE, 126(1), 57–62.
- Chen, Q., Kirby, J. T., Dalrymple, R. A., Kennedy, A. B., and Haller, M. C. (1999). "Boussinesq modelling of a rip current system." *J. Geophys. Res.*, 104(9), 20,617–20,637.
- Heitner, K. L., and Housner, G. W. (1970). "Numerical model for tsunami runup." *J. Wtrwy., Port, Coast., and Oc. Engrg.*, ASCE, 96, 701–719.
- Horikawa, K., and Kuo, C.-T. (1966). "A study on wave transformation inside surf zone." *Proc., Int. Conf. Coastal Eng.*, ASCE, New York, 217–233.
- Madsen, P. A., and Schäffer, H. A. (1998). "Higher order Boussinesq-type equations for surface gravity waves—Derivation and Analysis." *Philosophical Trans. Royal Soc.*, London, 356, 1–59.
- Madsen, P. A., and Sørensen, O. R. (1992). "A new form of the Boussinesq equations with improved linear dispersion characteristics. Part II: A slowly varying bathymetry." *Coast. Engrg.*, 18, 183–204.

- Madsen, P. A., Sørensen, O. R., and Schäffer, H. A. (1997a). "Surf zone dynamics simulated by a Boussinesq-type model. Part I: Model description and cross-shore motion of regular waves." *Coast. Engrg.*, 32, 255–287.
- Madsen, P. A., Sørensen, O. R., and Schäffer, H. A. (1997b). "Surf zone dynamics simulated by a Boussinesq-type model. Part II: Surf beat and swash oscillations for wave groups and irregular waves." *Coast. Engrg.*, 32, 289–319.
- Mase, H. (1995). "Frequency down-shift of swash oscillation compared to incident waves." *J. Hydr. Res.*, Delft, The Netherlands, 33(3), 397–411.
- Mase, H., and Kirby, J. T. (1992). "Hybrid frequency-domain KdV equation for random wave transformation." *Proc., 23rd Int. Conf. Coast. Eng.*, ASCE, New York, 474–487.
- Nwogu, O. (1993). "Alternative form of Boussinesq equations for near shore wave propagation." *J. Wtrwy., Port, Coast., and Oc. Engrg.*, ASCE, 119(6), 618–638.
- Özkan-Haller, H. T., and Kirby, J. T. (1997). "A Fourier-Chebyshev collocation method for the shallow water equations including shoreline runup." *Appl. Ocean Rs.*, 19, 21–34.
- Peregrine, D. H. (1967). "Long waves on a beach." *J. Fluid Mech.*, 27, Cambridge, England, 815–827.
- Schäffer, H. A., Madsen, P. A., and Deigaard, R. A. (1993). "A Boussinesq model for waves breaking in shallow water." *Coast. Engrg.*, 20, 185–202.
- Svendsen, I. A., Yu, K., and Veeramony, J. (1996). "A Boussinesq breaking wave model with vorticity." *Proc., 25th Int. Conf. Coastal Engrg.*, ASCE, New York, 1192–1204.
- Tao, J. (1983). "Computation of wave run-up and wave breaking." *Internal Rep.*, Danish Hydraulics Institute, Horsholm, Denmark.
- Tao, J. (1984). "Numerical modelling of wave runup and breaking on the beach." *Acta Oceanologica Sinica*, Beijing, 6(5), 692–700 (in Chinese).
- Wei, G., and Kirby, J. T. (1996). "A coastal processes model based on time-domain Boussinesq equations." *Res. Rep. No. CACR-96-01*, Center for Applied Coastal Research, Newark, Del.
- Wei, G., Kirby, J. T., Grilli, S. T., and Subramanya, R. (1995). "A fully nonlinear Boussinesq model for surface waves. I: Highly nonlinear, unsteady waves." *J. Fluid Mech.*, Cambridge, England, 294, 71–92.
- Wei, G., Kirby, J. T., and Sinha, A. (1999). "Generation of waves in Boussinesq models using a source function model." *Coast. Engrg.*, 36, 271–299.
- Zelt, J. A. (1991). "The run-up of nonbreaking and breaking solitary waves." *Coast. Engrg.*, 15, 205–246.